International Journal For Advanced Research In Science & Technology
A peer reviewed international journal
www.ijarst.in
ISSN: 2457-0362

Power Quality Enhancement of Wind Turbines Under Unbalanced Voltage Conditions using A Sliding Mode Approach

***Namburi Ramya*[1], CH Chinna Veera*i*[2]**

[1]PG Student, Dept of EEE, Amrita Sai Institute of Science and Technology (Autonomous).

[2]Associate Professor, Dept of EEE, Amrita Sai Institute of Science and Technology (Autonomous).

[1]ramyanamburi368@gmail.com.

***Abstract*—**An integral terminal sliding mode-based control design is proposed in this paper to enhance the power quality of wind turbines under unbalanced voltage conditions. The design combines the robustness, fast response, and high quality transient characteristics of the integral terminal sliding mode control with the estimation properties of disturbance observers. The controller gains were auto-tuned using a fuzzy logic approach. The effectiveness of the proposed design was assessed under deep voltage sag conditions and parameter variations. Its dynamic response was also compared to that of a standard SMC approach. The performance analysis and simulation results confirmed the ability of the proposed approach to maintain the active power, currents, DC-link voltage and electromagnetic torque within their acceptable ranges even under the most severe unbalanced voltage conditions. It was also shown to be robust to uncertainties and parameter variations, while effectively mitigating chattering in comparison with the standard SMC.

Index Terms—Doubly fed induction generators (DFIG), fuzzy approach, integral terminal sliding mode control (ITSMC), observer, power quality, voltage unbalances, wind turbines.

I. INTRODUCTION

ONE of the most challenging issues with wind energy nowadays is its integration into the power grid network [1]. Wind turbines are required to comply with several technical requirements and remain connected to the grid in the presence of different grid voltage disturbances such as voltage unbalances and harmonics [2]. Moreover, the amount of harmonics in the total current injected into the grid by the wind turbine is limited by the standard requirements [3]. Doubly fed induction generators (DFIG) are widely deployed in variable speed wind turbines. A challenging problem with DFIG's though is their extreme sensitivity to voltage fluctuations in the grid network. Even the smallest variations in grid voltages can lead to a sharp increase in stator and rotor currents which can cause damages to the DFIG's converters and deteriorate the wind turbine's output power quality [4]. Various approaches have traditionally been considered to protect wind turbines from the effects of voltage fluctuations. Crowbar circuits [5] are among the most common approaches. Nevertheless, DFIG typically absorbs large amounts of reactive power

International Journal For Advanced Research In Science & Technology
A peer reviewed international journal www.ijarst.in
ISSN: 2457-0362

during grid faults and crowbar circuits further aggravate this problem. Series dynamic resistors (SDR) [6] were also considered in voltage sag mitigation given their ability to keep rotor currents and stator voltages within acceptable ranges. In this condition, SDR hinclers the DFIG's ability to properly supply reactive power to the grid. Employing a shunt current injection approach or adding a STATCOM can compensate for the voltage unbalance at the point of common coupling (PCC) and cancel the swings in the electromagnetic torque [7], [8]. However, the STATCOM cannot decrease the over-voltages and overcurrents in DFIG's circuits. Series grid side converters (SGSC) [4] and dynamic voltage restorers (DVR) [9] are very effective at mitigating voltage unbalances, but, the required energy storage equipment to absorb the excess energy makes these approaches costly. Moreover, all the above mentioned measures are only effective when the voltage fluctuations are not deep. Various control approaches were introduced in the literature to properly control the rotor (RSC) and grid (GSC) side converters of the DFIG and mitigate grid voltage unbalances.Conventional PIs are among the most popular [10]. Which lack the necessary robustness against external disturbances, parametric uncertainties and un-modeled dynamics; ubiquitous problems in DFIG-based wind turbines. Sliding mode control (SMC) is widely considered as a powerful control approach for systems with uncertainties and/or unknown disturbances [11]. Features such robustness of the controlled system to both internal parameter uncertainties and external disturbances along with the relative ease of its implementation have led

to its consideration for a wide range of nonlinear uncertain systems [12]. Though there are several variants of SMC approaches [11]¡[17], this design typically consists of two stages: 1) a sliding phase during which a hyperplane, namely, sliding surface, is designed to provide the desired behavior for the closed-loop system during sliding mode, and 2) a reaching phase during which a discontinuous control law is designed to force all the trajectories to reach the sliding surface and remain on it. The sliding surface is also considered to be the switching

condition during the reaching phase design. As long as the sliding mode is realized, the SMC renders the system totally insensitive to parameter perturbations, un-modeled dynamics and external matched disturbances. A standard first order SMC approach was proposed in [18] for DFIG-based WTs. A sliding mode controller was proposed in [19] for the voltage regulation of a DFIG wind generator connected to the microgrid. The high-frequency switching or chattering phenomenon associated with standard

SMC, however, has the potential to excite the system's unmodeled dynamics, overheat the DFIG and lead to wear of the moving mechanical parts [13]. Further, although appropriate adjustment of the parameters may lead to an arbitrarily fast convergence rate, conventional SMC does not guarantee the

International Journal For Advanced Research In Science & Technology
A peer reviewed international journal www.ijarst.in
ISSN: 2457-0362

convergence of system dynamics in finite time. Moreover, it can only guarantee asymptotic stability in the sliding phase. Since stabilizing dynamical systems and ensuring error convergence in finite time is more desirable in practice, terminal sliding mode controls (TSMC) with nonlinear sliding hyperplanes were proposed to alleviate this drawback [11]. A TSMC scheme was proposed in [20] for the grid side converter of a DFIG-based wind turbine. However, TSMC suffers from the singularity problem and have restrictions on the range of fractional power functions [12]. The singularity problem will not happen however on the control law if Integral TSMC approaches are considered instead [13]. Further ITSMC designs
were shown to offer a better and enhanced transient response for a wide range of MIMO nonlinear systems [21]. An ITSMC approach was developed in [22] for the rotor side converter
of a DFIG-based WT. The comparison study reported in [23] showed that ITSMC outperformed the standard SMC when implemented to the RSC of a DFIG-based WT. This paper designs and implements an integral terminal sliding mode-based control approach for the rotor side and
grid side converters of a DFIG-based wind turbine. Its main contributions are as follows:

1) A control algorithm that combines the robustness, fast response, and transient characteristics of the ITSMC with the estimation properties of disturbance observers.

2) A control paradigm that maintains power quality in the presence of deep grid voltage unbalances and system disturbances.

3) A design that ensures chattering free dynamics in comparison to standard SMC.

The paper is organized as follows. The dynamic models of the converters are provided in Section II. The proposed disturbance observer ITSMDO is derived in Section III. Theproposed ITSMC controllers for both RSC and GSC are derived in Section IV. Performance evaluation of the proposed approach is carried out in Section V. Some concluding remarks are provided in Section VI.

II. MODELLING OF A DFIG-BASED WIND TURBINE

The schematic representation of a DFIG-based WT connected to the microgrid is depicted in Fig. 1.

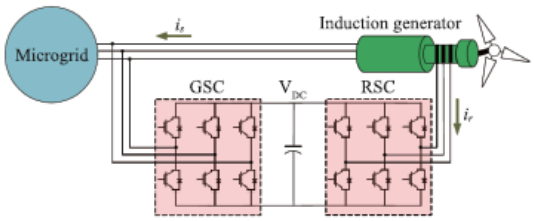

Fig. 1. Schematic diagram of a DFIG-based WT.

A. Modelling of the Rotor Side Converter

Assuming the system to be balanced and symmetrical, the state space model of the DFIG in the synchronously rotating reference frame (d ¡ q) [24] is represented by:

$$X = f(x; t) + g(x; t)\, u \qquad (1)$$

International Journal For Advanced Research In Science & Technology
A peer reviewed international journal
www.ijarst.in
ISSN: 2457-0362

where,

$f(x; t) =$

$$\begin{bmatrix} -\frac{R_r}{(\sigma L_r)^2}\left(\sigma L_r i_{r,d}+\frac{MV_{s,q}}{\omega_s L_s}\right)+\frac{R_r M\psi_{s,d}}{L_s(\sigma L_r)^2}+\frac{\omega_r}{\sigma L_r}\left(\sigma L_r i_{r,q}+\frac{MV_{s,d}}{\omega_s L_s}\right) \\ -\frac{R_r}{(\sigma L_r)^2}\left(\sigma L_r i_{r,q}+\frac{MV_{s,d}}{\omega_s L_s}\right)+\frac{R_r M\psi_{s,q}}{L_s(\sigma L_r)^2}-\frac{\omega_r}{\sigma L_r}\left(\sigma L_r i_{r,d}+\frac{MV_{s,q}}{\omega_s L_s}\right) \end{bmatrix}$$

$$g(x,t) = \begin{bmatrix} \frac{1}{\sigma L_r} & 0 \\ 0 & \frac{1}{\sigma L_r} \end{bmatrix}$$

The state vector is $X = [i_{r,d} \quad i_{r,q}]^T$ and the input vector is $[u_{r,d} \quad u_{r,q}]^T = [V_{r,d} \quad V_{r,q}]^T$ and $\sigma = 1 - \frac{M^2}{L_s L_r}$. By considering a reference frame synchronously rotating with the stator flux, we obtain

$$\psi_{s,d} = \psi_s, \psi_{s,q} = 0 \qquad (2)$$

and by neglecting the stator resistance, we have

$$V_{s,d} = 0; \; V_{s,q} = V_s = \omega_s \psi_s \qquad (3)$$

We can rewrite (1) as follows [24]:

2where $f(x; t) =$

$$\begin{bmatrix} \underbrace{-\frac{R_r}{(\sigma L_r)^2}\left(\sigma L_r i_{r,d}+\frac{MV_s}{\omega_s L_s}\right)+\frac{R_r M\psi_s}{L_s(\sigma L_r)^2}+\omega_r i_{r,q}}_{F_{r,d}} \\ \underbrace{-\frac{R_r}{\sigma L_r} i_{rq}-\frac{\omega_r}{\sigma L_r}\left(\sigma L_r i_{r,d}+\frac{M}{\omega_s L_s} V_{s,q}\right)}_{F_{r,q}} \end{bmatrix}$$

Hence,

$$\begin{cases} \dot{i}_{r,d} = F_{r,d} + G_{e,r,d} u_d + D_{r,d} \\ \dot{i}_{r,q} = F_{r,q} + G_{e,r,q} u_q + D_{r,q} \end{cases} \qquad (5)$$

Where $G_{e,r,d} = G_{e,r,q} = \frac{1}{\sigma L_r}$. $Dr;d$ and $Dr;q$ are assumed to be bounded with $D_{r,j} \leq \Upsilon_{r,j}$, $j = d; q$ [25].

B. Modelling of the Grid Side Converter

Grid side converters are instrumental in regulating the DCDC- link voltage of DFIGs and decreasing the swings of the total active and reactive power injected to the grid. However, proper control of the GSC is necessary to maintain constant DC voltage and enhance power quality under unbalanced grid conditions. The GSC can be modeled in the d ¡ q frame by

$$\begin{cases} \frac{di_{g,d}}{dt} = \underbrace{\frac{1}{L_g}(V_{s,d} - R_g i_{g,d} + \omega_s L_g i_{g,q})}_{F_{g,d}} - \frac{1}{L_g} V_{g,d} \\ \frac{di_{g,q}}{dt} = \underbrace{\frac{1}{L_g}(V_{s,q} - R_g i_{g,q} - \omega_s L_g i_{g,d})}_{F_{g,q}} - \frac{1}{L_g} V_{g,q} \end{cases} \qquad (6)$$

Equation (6) can be re-written as follows:

$$\begin{cases} \dot{i}_{g,d} = F_{g,d} + G_{e,g,d} u_{g,d} + D_{g,d} \\ \dot{i}_{g,q} = F_{g,q} + G_{e,g,q} u_{g,q} + D_{g,q} \end{cases} \qquad (7)$$

where

$[u_{g,d} \quad u_{g,q}]^T = [V_{g,d} \quad V_{g,q}]^T$. $G_{e,g,d} = G_{e,g,q} = \frac{-1}{L_g}$. $D_{g,d}$ and $Dg;q$ are unknown but bounded lumped uncertainties with $\|D_{g,j}\| \leq \Upsilon_{g,j}$, $j = d; q$. For the above DFIGbased WT, we propose a robust control approach which is capable of mitigating faults, handling disturbances and parameter variations, while maintaining the currents and electromagnetic torque within acceptable ranges.

III. SLIDING MODE DISTURBANCE OBSERVER

To properly estimate the system's external disturbances, unmodeled dynamics and uncertainties, we design an integral terminal sliding mode disturbance observer

International Journal For Advanced Research In Science & Technology
A peer reviewed international journal www.ijarst.in
IJARST
ISSN: 2457-0362

(ITSMDO). Consider the following auxiliary variable

$$z_{k,j} = \sigma_{k,j} + \rho_{k,j} e_{I,k,j}, \quad j = d,\ q, k = r, g \qquad (8)$$

Where $\rho_{k,j}$ is a positive constant. *j = d; q* denotes the direct, quadrature components, and *k = r; g* refers to the rotor, grid side converter. The following variables are defined as follows:

$$\begin{cases} \sigma_{k,j} = i_{k,j} - h_{k,j} \\ \dot{h}_{k,j} = F_{k,j} + G_{e,k,j} u_{k,j} + \hat{D}_{k,j} \\ \dot{e}_{I,k,j} = \text{sign}(\sigma_{k,j}) \end{cases} \qquad (9)$$

where *eI;k;j* has the initial value $\frac{-\sigma_{k,j}(0)}{\rho_{k,j} \cdot e_{I,k,j}}$ converges to zero in the finite time $T_{S,k,j} = \frac{|\sigma_{k,j}(0)|}{\rho_{k,j}}$ [26].

The disturbance estimation $\hat{D}_{k,j}$ is calculated using $\sigma_{k,j} = 0$ as follows:

$$\hat{D}_{k,j} = \theta_{1,k,j} z_{k,j} + \theta_{2,k,j} \text{sign}(z_{k,j}) + \rho_{k,j} \text{sign}(\sigma_{k,j}) \qquad (10)$$

where $\theta_{1,k,j}$ and $\theta_{2,k,j} > \Upsilon_{k,j}$ are constant positive coefficients.

Theorem 1: For the system (1) and with the assumption $\|D_{k,j}\| \leq \Upsilon_{k,j}$, the ITSMDO designed illustrated in (8)–(10), yields auxiliary errors $\sigma_{k,j}$ and $e_{I,k,j}$ that converge to zero in finite time [25].

Proof: The first derivative of (8) is calculated as follows:

$$\dot{z}_{k,j} = \dot{\sigma}_{k,j} + \rho_{k,j} \dot{e}_{I,k,j} = \dot{i}_{k,d} - \dot{h}_{k,j} + \rho_{k,j} \text{sign}(\sigma_{k,j}) \qquad (11)$$

Substituting (5), (9) and (10) in (11), results in:

$$\dot{z}_{k,j} = D_{k,j} - \theta_{1,k,j} z_{k,j} - \theta_{2,k,j} \text{sign}(z_{k,j}) \qquad (12)$$

Considering the following Lyapunov function [27]:

$$E_{k,j} = \frac{1}{2} z_{k,j}^2 \qquad (13)$$

Computing the time derivative of, yields

$$\dot{E}_j = z_{k,j} \dot{z}_{k,j} < 0 \qquad (14)$$

Substituting (11) into (14) provides

$$\begin{aligned} \dot{E}_{k,j} &= z_{k,j} \left(D_{k,j} - \theta_{1,k,j} z_{k,j} - \theta_{2,k,j} \text{sign}(z_{k,j}) \right) \\ &\leq z_{k,j} D_{k,j} - \theta_{1,k,j} z_{k,j} z_{k,j} - \theta_{2,k,j} z_{k,j} \text{sign}(z_{k,j}) \\ &\leq \Upsilon_{k,j} \|z_{k,j}\| - \theta_{1,k,j} \|z_{k,j}\|^2 - \theta_{2,k,j} \|z_{k,j}\| \end{aligned} \qquad (15)$$

Given the fact that $\theta_{1,k,j} > \Upsilon_j$, we have

$$\dot{E}_{k,j} \leq -\theta_{1,k,j} \|z_{k,j}\|^2 = -2\theta_{1,k,j} E_{k,j}. \qquad (16)$$

Therefore, the auxiliary sliding vector of the ITSMDO (*zk;j*)is always kept on the surface *zk;j* = 0. Consequently, the auxiliary errors *¾k;j* and *eI;k;j* are guaranteed to converge in finite-time. It is very important to note that *μ2;k;j* must be tuned adaptively to prevent unstable conditions from happening.

Invoking (5), (8) and (9), we obtain

$$\begin{aligned} \tilde{D}_{k,j} &= \hat{D}_{k,j} - D_{k,j} \\ &= \hat{D}_{k,j} - \dot{i}_{k,d} + F_{k,j} + G_{e,k,j} u_{k,j} = -\dot{\sigma}_{k,j} \end{aligned} \qquad (17)$$

The finite time convergence property of the auxiliary variable *¾k;j* , yields the finite time convergence of the disturbance approximation error e*D*

Remark 1: The observer design requires knowledge of the upper boundary *¨k;j* of the dynamic errors. Since calculating *¨k;j* is quite complex, the approach outlined in [28] can be considered to properly calculate the adaptive gains *μ2;k;j* in (10).

Remark 2: The main feature of the ITSMDO is its convergence in the finite time (*TS;k;j*), thus eliminating the singularity problem encountered in traditional SMC approaches [12].

IV. DESIGN OF THE ITSMC-BASED APPROACH

A. ITSMC Design for the RSC and GSC

Define the tracking errors of the *d ¡ q* components of the

rotor and grid side currents (*sk;j*)as follows:

$$s_{k,j} = i_{k,j-ref} - i_{k,j} \qquad (18)$$

where *ik;j¡ref ; j = d; q; k = r; g* are the (*d ¡ q*) components of the reference values for the rotor and grid side currents. Note that, since the converter operates in a stator-flux *d; q*- reference frame, the rotor currents are decomposed into an active power (*d*-axis) and a reactive power (*q*-axis) component. The actual active power of the generator is compared with the reference point value,

International Journal For Advanced Research In Science & Technology
A peer reviewed international journal www.ijarst.in
IJARST
ISSN: 2457-0362

which is determined by the wind speed. The difference between these two values will be fed to the controller which in turn will use it to generate the reference value of the *d*-axis rotor current *ir;d¡ref* . Likewise, actual reactive power of the generator is compared with the reference point value (usually considered zero). The difference between these two values will go to a controller, which is used to generate the reference value of the *q*-axis rotor current *ir;q¡ref* . The first derivative of (18) can be written as follows:

$$\dot{s}_{k,j}(t) = \dot{i}_{k,j-ref} - \dot{i}_{k,j} \tag{19}$$

Substituting either (5) (RSC) or (7) (GCS) in (19), yields:

$$\dot{s}_{k,j}(t) = \underbrace{\dot{i}_{k,j-ref} - F_{k,j}}_{\Lambda_{k,j}} + \hat{D}_{k,j} - G_{e,k,j}u_{k,j}. \tag{20}$$

The sliding surfaces of the $(d-q)$ components of the rotor current $(S_{k,j})$ are defined as follows:

$$S_{k,j} = s_{k,j} + \beta_{1,k,j}e_{I,k,j}s_{k,j} + \beta_{2,k,j}\left(s_{k,j}{}^2\right)^{-\alpha_k} s_{k,j}e^{-\lambda_k t} \tag{21}$$

where $\alpha_k, \lambda_k, \beta_{1,k,j}$ and $\beta_{2,k,j}$ are positive constants. $e_{I,k,j}(t) = \int \text{sign}(s_{k,j}(t))dt$ are respectively the sign integrations of the tracking error's d and q components. Deriving (19) and using (18) yields:

$$\dot{S}_{k,j} = \xi_{1,k,j}\left(\Lambda_{k,j} + \hat{D}_{k,j} - G_{e,k,j}u_{k,j}\right) + \xi_{2,k,j}s_j + \xi_{3,k,j}. \tag{22}$$

The following coefficients are computed as follows:

$$\begin{cases} \xi_{1,k,j} = 1 + \beta_{1,k,j}e_{I,k,j} - \beta_{2,k,j}(2\alpha_k - 1)e^{-\lambda_k t}s_{k,j}{}^{-2\alpha_k} \\ \xi_{2,k,j} = \beta_{1,k,j}\dot{e}_{I,k,j} \\ \xi_{3,k,j} = -\beta_{2,k,j}\lambda_k s_{k,j}{}^{-2\alpha_k+1}e^{-\lambda_k t} \end{cases} \tag{23}$$

Maintaining the output trajectory on the sliding surface entails fulfilling the following necessary condition: *_S k;j* (*t*) = 0*; j* = *d; q*[29]

$$\dot{S}_{k,j}(t) = 0,\ j = d,\ q$$
$$\dot{S}_{k,j} = \xi_{1,k,j}\left(\Lambda_{k,j} + \hat{D}_{k,j} - G_{e,k,j}u_{k,j}\right) + \xi_{2,k,}$$
$$+ \xi_{3,k,j} = 0.$$

Theorem 2: Asymptotic convergence of the tracking error (18) to zero will be guaranteed by selecting the surfaces (21) and designing the control law as follows [30]:

$$u_{k,j}(t) = u_{eq,k,j} + u_{p,k,j} \tag{25}$$

where $u_{eq,k,j}$ is defined by $\dot{S}_{k,j}(t) = 0$ as follows:

$$u_{eq,k,j} = \left(G_{e,k,j}\xi_{1,k,j}\right)^{-1}\left(\xi_{2,k,j}s_{k,j} + \xi_{3,k,j} + \xi_{1,k,j}\left(\Lambda_{k,j} + \hat{D}_{k,j}\right)\right) \tag{26}$$

$u_{p,k,j}$ can be defined as follows:

$$u_{p,k,j} = \left(G_{e,k,j}\xi_{1,k,j}\right)^{-1}\left(K_{1,k,j}s_{k,j} + K_{2,k,j}\text{sign}(s_{k,j})\right) \tag{27}$$

where $K_{1,k,j}$ and $K_{2,k,j}$ are positive constants.

B. Computation of the Convergence Time of the ITSMC

Theorem 3: The sliding mode surfaces will converge in finite time if $2\xi_{1,k,j}^{-1}\beta_{1,k,j}e_{I,k,j} - \lambda_k > 0$.

Proof:

$$V_{k,j} = \frac{1}{2}s_{k,j}^2 \tag{28}$$

Computing the time derivative of $V_{k,j}$

$$\dot{V}_{k,j} = s_{k,j}\dot{s}_{k,j} < 0 \tag{29}$$

$\dot{S}_{k,j}(t) = 0$, yields

$$\dot{S}_{k,j} = \xi_{1,k,j}\dot{s}_{k,j} + \beta_{1,k,j}\dot{e}_{I,k,j}s_{k,j} - \beta_{2,k,j}\lambda_k s_{k,j}{}^{-2\alpha_k+1}e^{-\lambda_k t} = 0. \tag{30}$$

Hence

$$\dot{s}_{k,j} = -\xi_{1,k,j}^{-1}\beta_{1,k,j}e_{I,k,j}s_{k,j} + \xi_{1,k,j}^{-1}\beta_{2,k,j}\left(s_{k,j}{}^2\right)^{-\alpha_k}s_{k,j}e^{-\lambda_k t}. \tag{31}$$

Substituting (31) into (29) provides

$$\dot{V}_{k,j} = -\xi_{1,k,j}^{-1}\beta_{1,k,j}e_{I,k,j}s_{k,j}^2 + \xi_{1,k,j}^{-1}\beta_{2,k,j}s_{k,j}^{2(1-\alpha_k)}e^{-\lambda_k t}. \tag{32}$$

Considering (28), yields

$$\dot{V}_{k,j} = -2\xi_{1,k,j}^{-1}\beta_{1,k,j}e_{I,k,j}V_{k,j} + 2^{1-\alpha_k}\xi_{1,k,j}^{-1}\beta_{2,k,j}V_{k,j}^{1-\alpha_k}e^{-\lambda_k t}. \tag{33}$$

Multiplying both sides of (31) by $\alpha\ V_{k,j}^{\alpha-1}$, yields

$$\dot{V}_{k,j}^{\alpha_k} + 2\xi_{1,k,j}^{-1}\beta_{1,k,j}e_{I,k,j}V_{k,j}^{\alpha_k} = 2^{1-\alpha_k}\alpha_k\xi_{1,k,j}^{-1}\beta_{2,k,j}e^{-\lambda_k t}. \tag{34}$$

Integrating (34) from 0 to $T_{S,k,j}$ and considering the fact that $V_{k,j}(T_{S,k,j}) = 0$, yields the following convergence time $T_{S,k,j}$:

$$T_{S,k,j} = \frac{Ln\left(1 - \Omega_{k,j}V_{k,j}^{\alpha_k}(0)\right)}{2\xi_{1,k,j}^{-1}\beta_{1,k,j}e_{I,k,j} - \lambda_k} \tag{35}$$

where the coefficients *-k;j* are calculated as follows:

$$\Omega_{k,j} = \frac{2^{1-\alpha_k}\alpha_k\xi_{1,k,j}^{-1}\beta_{2,vj}}{2\xi_{1,k,j}^{-1}\beta_{1,k,j}e_{I,k,j} - \lambda_k}. \tag{36}$$

International Journal For Advanced Research In Science & Technology
A peer reviewed international journal
www.ijarst.in
ISSN: 2457-0362

Remark 3: The term $(e^{-\lambda_k t})$ will converge to zero after a certain time, thus rendering the sliding surface linear thereafter.

C. Stability Analysis

Considering the following Lyapunov function [27]:

$$L_{k,j} = \frac{1}{2} S_{k,j}^2 \tag{37}$$

Calculating the time derivative of $L_{k,j}$ as follows:

$$\dot{L}_{k,j} = S_{k,j} \dot{S}_{k,j} < 0. \tag{38}$$

Substituting (22) and (25) into (38), yields

$$\dot{L}_{k,j} = S_{k,j} \left\{ \xi_{1,k,j} \left(\Lambda_{k,j} + D_{k,j} - G_{e,k,j} u_{k,j} \right) + \xi_{2,k,j} s_{k,j} + \xi_{3,k,j} \right\}. \tag{39}$$

Substituting (26) and (27) into (39) provides

$$\begin{aligned} \dot{L}_{k,j} &= S_{k,j} \xi_{1,k,j} (D_{k,j} - \hat{D}_{k,j}) - K_{1,k,j} |S_{k,j}|^2 \\ &\quad - K_{2,k,j} |S_{k,j}| < 0 \\ &\leq |S_{k,j}| \xi_{1,k,j} \dot{\sigma}_{k,j} - K_{1,k,j} |S_{k,j}|^2 - K_{2,k,j} |S_{k,j}|. \end{aligned} \tag{40}$$

It is assumed that $K_{2,k,j} > \xi_{1,k,j} \dot{\sigma}_{k,j}$. Hence, we have

$$\dot{L}_{k,j} \leq -K_{1,k,j} |S_{k,j}|^2 - K_{2,k,j} |S_{k,j}| < 0. \tag{41}$$

Thus the finite time convergence of $S(t)$ to zero is guaranteed.

D. Gain Auto-tuning via a Fuzzy Approach

To ensure self-adaptation, a fuzzy approach was designed to auto-tune the parameters of the ITSMC controller. The parameters of the ITSMC controller ´*i; i* = 1*; : : : ;* 8 $(\beta_{1,k,j}, \beta_{2,k,j})$ were adjusted and tuned by ¢´*i* as illustrated in Fig. 2. The considered fuzzy logic rules for ¢´*i* are illustrated in Table I in the Appendix. Note that, the controller parameters are adjusted based on the tracking errors of the *d¡q* components of the rotor currents (*Sdq*). The tuned variables are thus calculated as follows:

$$\text{Tuned Variable} = \eta_i + \Delta\eta_i, i = 1, \ldots, 8. \tag{42}$$

The membership functions for the fuzzy logic controller are illustrated in Fig. 3. They involve seven segments, including zero (ZO), negative small (NS), negative medium (NM), negative big (NB), positive small (PS), positive medium (PM) and positive big (PB). The range of inputs s_j and Δs_j and based on Fig. 3 is $\{-1, -\frac{2}{3}, -\frac{1}{3}, 0, \frac{1}{3}, \frac{2}{3}, 1\}$, while the range of outputs $\Delta\eta_i$ is $\{-0.6, -0.3, -0.1, 0, 0.1, 0.3, 0.6\}$.

Fig. 4 illustrates the block diagram of the overall control structure.

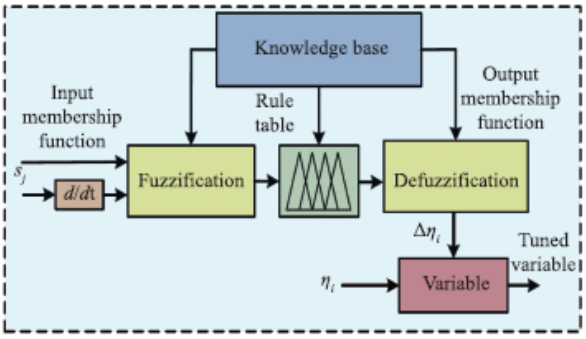

Fig. 2. Structure of the fuzzy approach.

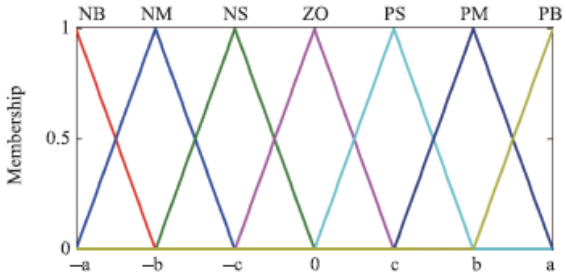

Fig. 3. Membership functions of the fuzzy logic approach.

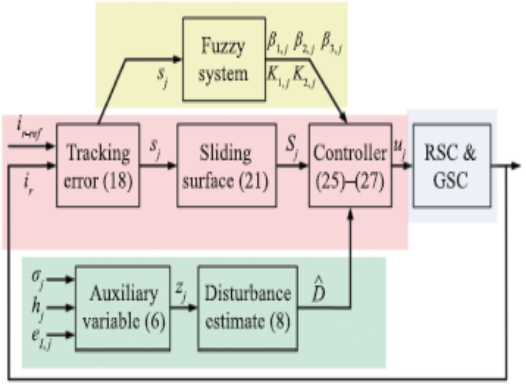

Fig. 4. Block diagram of the control structure.

International Journal For Advanced Research In Science & Technology
A peer reviewed international journal
www.ijarst.in
ISSN: 2457-0362

V. PERFORMANCE EVALUATION

To assess the performance of the proposed design, we implemented it to a DFIG-based WT connected to the microgrid topography highlighted in [31]. The schematic diagram of the controlled system is illustrated in Fig. 5. The parameters of the considered wind turbine are listed in Table II in the Appendix.

A. DFIG Performance Using the Proposed Approach Under Voltage Sag Conditions

Voltage sags are the most frequent grid faults and the leading cause for power quality problems [32]¡[34]. These are short duration reductions in rms voltage ranging from 10 to 90 percent [6]. If not properly mitigated, they usually result in sudden increase in the transient currents, which in turn result in poor power quality, soaring the ratings of the semiconductor devices and potentially damage the converters. The resulting current fluctuations and potential damages increase with the severity of the voltage sag. As a protective measure, WTs must be disconnected from the grid when the resulting current harmonics exceed converters rates, as defined by the grid code requirements [2] and the IEEE standards for harmonic control in electric power systems [3].

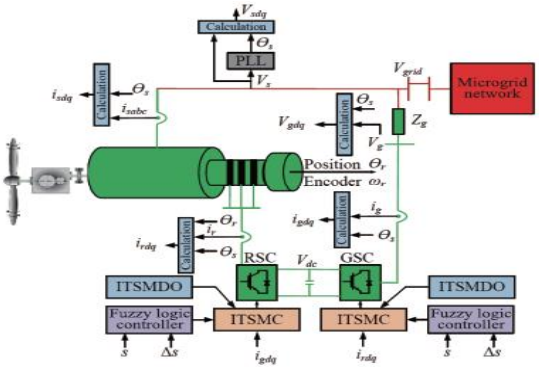

Fig. 5. Schematic diagram of the controlled system.

To assess the ability of the proposed control algorithm to mitigate voltage sags and prevent WTs from being disconnected from the grid, we performed tests under worst case scenario. Thereby, a voltage sag of 80% magnitude was injected to the grid network between t =0.5 and t =0.7 s. The DFIG's stator voltage, stator and rotor currents in this case are depicted in Figs. 6 (a)¡(c). The time histories of the active power, DC-link voltage and electromagnetic torque in this case are illustrated in Figs. 7 (a)¡(c).

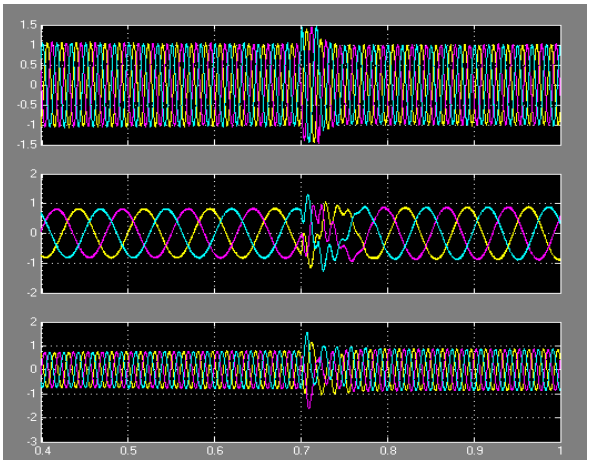

Fig. 6. (a) Stator voltage (pu), (b) rotor current (pu), (c) stator current (pu) of DFIG-based WT (proposed approach).

International Journal For Advanced Research In Science & Technology
A peer reviewed international journal
www.ijarst.in
IJARST
ISSN: 2457-0362

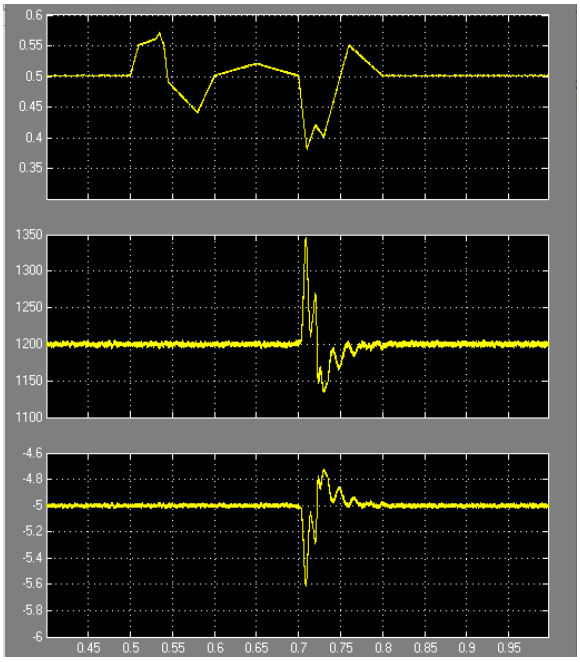

Fig. 7. DFIG's (a) Active power (pu), (b) DC-link voltage (V), (c) Electromagnetic torque (pu) (proposed approach).

Note that the harmonics observed in the stator and rotor currents during the voltage sag are within the range. Note also
the smooth and chattering free dynamics observed with all the variables. Thus, despite the severity of the voltage sag, the active power, currents, DC link voltage and electromagnetic torque remained within their acceptable ranges. The obtained results thus confirm the effectiveness of the proposed control algorithm in riding through deep voltage sags and maintaining power quality no matter the depth of the voltage unbalance. Figs. 8 (a)¡(b) depict the dynamics of the sliding surfaces considered in the proposed FSOITSMC approach.

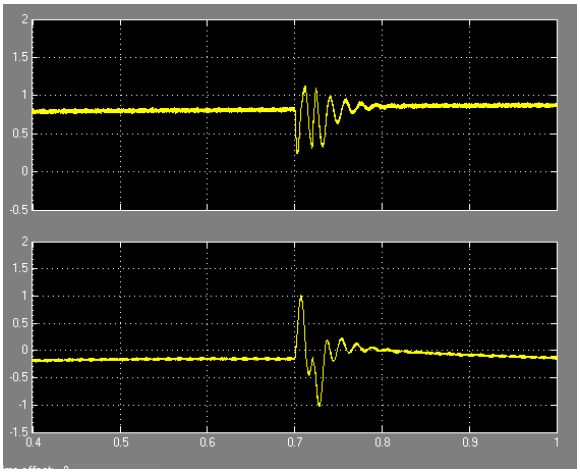

Fig. 8. Sliding surface of (a) *d*, and (b) *q* components of rotor current (proposed approach).

Note the increase in sliding surface magnitude to compensate for the voltage sag when this later happens. However, despite the severity of the voltage sag, the overall magnitude and frequency of the sliding surfaces remained reasonable.

B. Comparison With a Standard SMC Approach

To further assess the performance of the proposed control strategy, we compared our results with those obtained using the standard SMC design proposed in [35]. Under the same conditions as the ones considered in Section V-A, the SSMC yielded the stator voltage, and rotor and stator currents depicted
in Figs. 9 (a)¡(b). It also generated the active power, DC-link voltage and electromagnetic torque depicted in Fig.10. Note the relatively high magnitude of the fluctuations in the respective variables during the sag conditions, when considering the SSMC.The

International Journal For Advanced Research In Science & Technology
A peer reviewed international journal
www.ijarst.in
IJARST
ISSN: 2457-0362

sliding surfaces of the SSMC approach are depicted in Figs. 11 (a)¡(b). Note that the SSMC requires sliding surfaces with much higher frequency and larger magnitudes to achieve the same control targets. Note also the chattering in the dynamics of the power, DC voltage, currents and electromagnetic torque when considering the SSMC, whereas our approach yielded quasi-chattering free performance for the same conditions.

C. Robustness to Parameter Variations

In addition to the conditions considered in Section V-A, the DFIG was subjected to a 20% increase in the rotor and stator resistances and inductances. The results obtained in this case were compared to those obtained with the nominal parameters. The DC-link voltage and active power of the DFIG in the presence of parameter variations are illustrated in Figs. 12 (a)¡(b). The results are compared to those obtained with the nominal parameters.

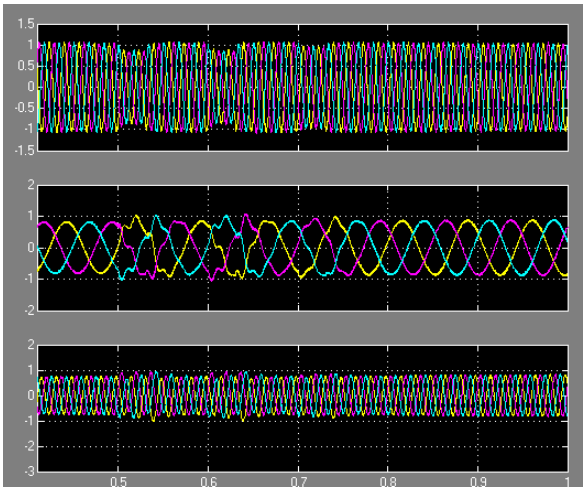

Fig. 9. (a) Stator voltage (pu), (b) rotor current (pu), (c) stator current (pu) of DFIG-based WT (SSMC).

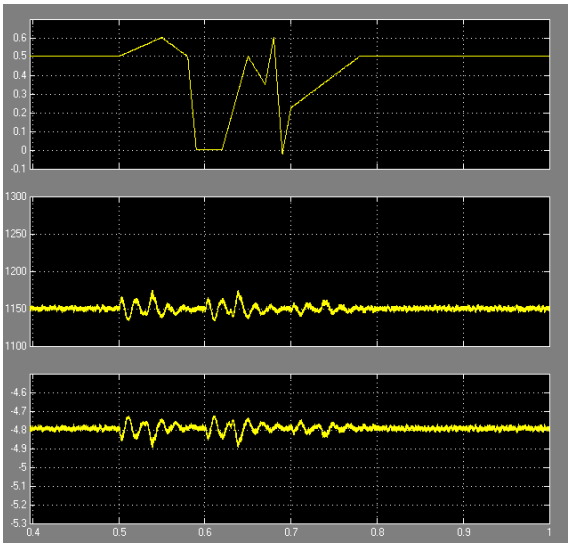

Fig. 10. DFIG's (a) Active power (pu), (b) DC-link voltage (V), and (c) Electromagnetic torque (pu) (SSMC).

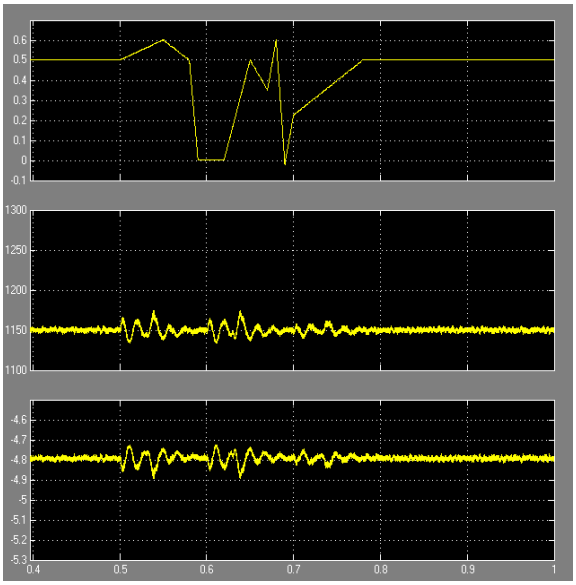

Fig. 11. DFIG's (a) Active power (pu), (b) DC-link voltage (V), and (c) Electromagnetic torque (pu) (SSMC).

International Journal For Advanced Research In Science & Technology
A peer reviewed international journal
www.ijarst.in
IJARST
ISSN: 2457-0362

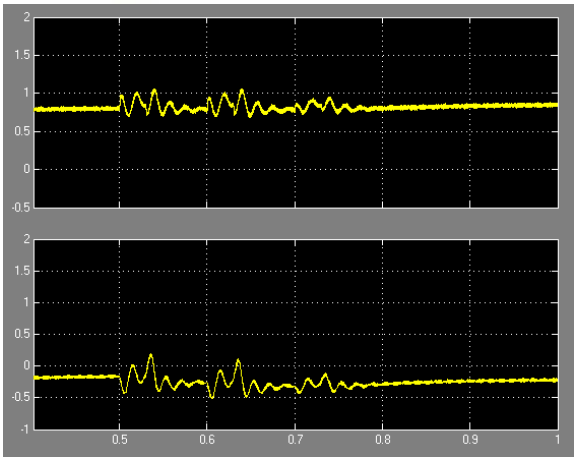

Fig. 12. DFIG's (a) DC-link voltage (V), and (b) Electromagnetic torque (pu) (proposed approach).

Note that the dynamic behavior of the DC-link voltage and electromagnetic torque barely vary as a result of the parameter variations. This confirms the robustness properties of the proposed control approach and asserts that the proposed ITSMDO is excellent at estimating the disturbances. For comparison purposes, we performed the same experiments with the SSMC approach proposed in [35]. The obtained results are illustrated in Fig. 13.

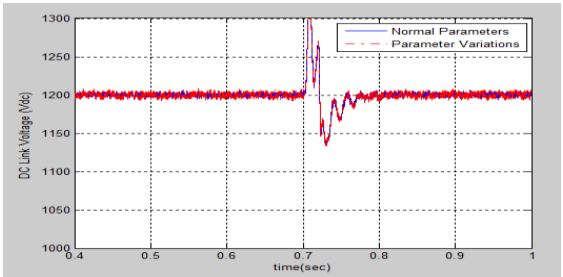

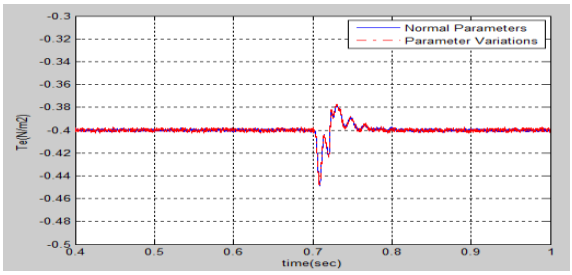

Fig. 13. DFIG's (a) DC-link voltage (V), (b) Electromagnetic torque (pu) (SSMC).

Note the differences in the dynamics between the results obtained under parameter variations and those with the nominal parameters. Note also the magnitude of the chattering in this case. Thus, all the results depicted in this section clearly highlight the superior performance of the proposed approach compared to the SSMC. They also confirm its ability to yield chattering free dynamics compared to the SSMC. This feature is quite important since the sudden and rapid fluctuations resulting from the chattering phenomena can damage the converters and deteriorate power quality [36].

VI. CONCLUSION

This paper proposed and implemented a novel ITSMCbased approach for grid-connected wind turbine subject to unbalanced voltage conditions and and disturbances. The approach combined the estimation accuracy of disturbance observers with the robustness and finite time convergence of the integral terminal sliding mode control. It was successfully implemented to both the rotor-side (RSC) and grid side (GSC)

International Journal For Advanced Research In Science & Technology
A peer reviewed international journal www.ijarst.in
ISSN: 2457-0362

converters of a DFIG-based wind turbine. Its performance was assessed in the presence of deep voltage sags and under varying parameter conditions. It was also compared to that of the standard SMC. The proposed approach was effective in maintaining the currents, DC-link voltages and electromagnetic
torque within their acceptable ranges even under the most severe voltage imbalances. It was also shown to be robust to uncertainties and parameter variations. Note that without proper control, such severe voltage unbalances would otherwise lead to disconnecting the DFIG from the grid as a protective measure. The proposed approach would prevent that from happening and ensure the uninterrupted service of the wind energy system.

APPENDIX

TABLE I
CONTROL RULES FOR $\Delta\eta_i$

		s						
		PB	PM	PS	Z	NS	NM	NB
s	PB	NB	NB	NM	NM	NM	ZO	ZO
	PM	PB	PB	PM	PS	PS	ZO	ZO
	PS	PB	PM	PS	PS	ZO	NS	NM
	Z	PM	PM	PS	ZO	NS	NM	NM
	NS	PS	PS	ZO	NS	NS	NM	NB
	NM	ZO	ZO	NS	NS	NM	NB	NB
	NB	ZO	ZO	NS	NM	NM	NB	NB

TABLE II
DFIG PARAMETERS

Parameter	Value
Induction Generator (DFIG)	
Nominal Power/ Voltage/Frequency	4.5 (MW)/575 (V)/60 (Hz)
Pairs of Pole	3
Rs / Ls / M	0.007060(pu)/0.1710(pu)/2.9000 (pu)
Rr / Lr	0.0050 (pu)/0.156 (pu)
Rg / Lg	0.19838 (mΩ)/ 0.052621 (mH)
DC-link (DFIG)	
Nominal voltage/Capacitor of DC-link	1200(V)/ 0.03 (F)

REFERENCES

[1] T. Ackermann and P. E. Morthorst, "Economic aspects of wind power in power systems," *Wind Power in Power Systems*, pp. 383, 2005.
[2] M. Tsili and S. Papathanassiou, "A review of grid code technical requirements for wind farms," *IET Renewable Power Generation*, vol.
3, no. 3, pp. 308¡332, Sep. 2009. [3] "IEEE std. 519-2014: IEEE draft recommended practices and requirements
for harmonic control in electric power systems," *IEEE P519/D6ba, September 2013* pp. 1¡26, Nov 2013.
[4] J. Yao, H. Li, Z. Chen, X. Xia, X. Chen, Q. Li, and Y. Liao, "Enhanced control of a DFIG-based wind-power generation system with series grid-side converter under unbalanced grid voltage conditions," *IEEE Transactions on Power Electronics*, vol. 28, no. 7, pp. 3167¡3181, July 2013.
[5] S. Seman, J. Niiranen, and A. Arkkio, "Ride-through analysis of doubly fed induction wind-power generator under unsymmetrical network disturbance," *IEEE Transactions on Power Systems*, vol. 21, no. 4, pp. 1782¡1789, Nov. 2006.
[6] S. Zhang, K. Tseng, S. S. Choi, T. D. Nguyen, and D. L. Yao, "Advanced control of series voltage compensation to enhance wind turbine ride through," *EEE Transactions on Power Electronics*, vol. 27, no. 2, pp. 763¡772, Feb 2012.
[7] S. W. Mohod and M. V. Aware, "A STATCOM-control scheme for grid connected wind energy system for power quality improvement," *IEEE Systems Journal*, vol. 4, no. 3, pp. 346¡352, Sep. 2010.
[8] M. Edrah, K. L. Lo, and O. Anaya-Lara, "Impacts of high penetration of DFIG wind turbines on rotor angle stability of power systems," *IEEE Transactions on Sustainable Energy*, vol. 6, no. 3, pp. 759¡766, July 2015.
[9] C. Wessels, F. Gebhardt, and F. W. Fuchs, "Fault ride-through of a DFIG wind turbine using a dynamic voltage restorer during symmetrical and asymmetrical grid faults," *IEEE Transactions on Power Electronics*, vol. 26, no. 3, pp. 807¡815, March 2011.
[10] Y. Zhou, P. Bauer, J. A. Ferreira, and J. Pierik, "Operation of gridconnected DFIG under unbalanced grid voltage condition," *IEEE Transactions on Energy Conversion*, vol. 24, no. 1, pp. 240¡246, March 2009.
[11] B. Bandyopadhyay, S. Janardhanan, and S. K. Spurgeon, "Advances in sliding mode control," *Lecture Notes in Control and Information Sciences*, vol. 440, 2013.
[12] N. Derbel, J. Ghommam, and Q. Zhu, *Applications of Sliding Mode Control*. Springer 2017, vol. 79.
[13] M. T. Hamayun, C. Edwards, H. Alwi *et al.*, *Fault Tolerant Control Schemes Using Integral Sliding Modes*, Springer 2016.

[14] B. Beltran, T. Ahmed-Ali, and M. E. H. Benbouzid, "High-order sliding mode control of variable-speed wind turbines," *IEEE Transactions on Industrial electronics*, vol. 56, no. 9, pp. 3314¡3321, 2009.

[15] S. E. B. Elghali, M. E. H. Benbouzid, T. Ahmed-Ali, and J. F. Charpentier,"High-order sliding mode control of a marine current turbine driven doubly-fed induction generator," *IEEE Journal of Oceanic Engineering*, vol. 35, no. 2, pp. 402¡411, 2010.

[16] L. Xiong, J. Wang, X. Mi, and M. W Khan, "Fractional order sliding mode based direct power control of grid-connected DFIG," *IEEE Transactions on Power Systems*, vol. 33, no. 3, pp. 3087¡3096, 2018.

[17] N. Ullah, M. A. Ali, A. Ibeas, and J. Herrera, "Adaptive fractional order terminal sliding mode control of a doubly fed induction generator-based wind energy system," *IEEE Access*, vol. 5, pp. 21368¡21381, 2017.

[18] H. Amimeur, D. Aouzellag, R. Abdessemed, and K. Ghedamsi, "Sliding mode control of a dual-stator induction generator for wind energy conversion systems," *International Journal of Electrical Power & Energy Systems*, vol. 42, no. 1, pp. 60¡70, 2012.

[19] R. Aghatehrani and R. Kavasseri, "Sensitivity-analysis-based sliding mode control for voltage regulation in microgrids," *IEEE Trans. Sustain. Energy*, vol. 4, no. 1, pp. 50¡57, 2013.

[20] B. Chen, Y, Feng, and M. Zhou, "Terminal sliding-mode control scheme for grid-side PWM converter of DFIG-based wind power system," in *Proc. 39th Annual Conference of the IEEE Industrial Electronics Society*, 2013, pp. 8014¡8018.

[21] C.-S. Chiu, "Derivative and integral terminal sliding mode control for a class of MIMO nonlinear systems," *Automatica*, vol. 48, no. 2, pp. 316¡326, 2012.

[22] M. J. Morshed and A. Fekih, "Integral terminal sliding mode control to provide fault ride-through capability to a grid connected wind turbine driven DFIG," in *Proc. IEEE International Conference on Industrial Technology*, 2015, pp. 1059¡1064.

[23] M. J. Morshed and A. Fekih, "A comparison study between two sliding mode based controls for voltage sag mitigation in grid connected wind turbines," in *Proc. IEEE Conference on Control Applications*, 2015, pp. 1913¡1918.

[24] A. Abdou, A. Abu-Siada, and H. Pota, "Impact of vsc faults on dynamic performance and low voltage ride through of DFIG," *International Journal of Electrical Power & Energy Systems*, vol. 65, pp. 334¡347,2015.

[25] W.-H. Chen, J. Yang, L. Guo, and S. Li, "Disturbance-observer-based control and related methodsan overview," *IEEE Transactions on Industrial Electronics*, vol. 63, no. 2, pp. 1083¡1095, 2016.

[26] L. Qiao and W. Zhang, "Adaptive non-singular integral terminal sliding mode tracking control for autonomous underwater vehicles," *IET Control Theory & Applications*, vol. 11, no. 8, pp. 1293¡1306, 2017.

[27] F.-J. Lin, Y.-C. Hung, and K.-C. Ruan, "An intelligent second-order sliding-mode control for an electric power steering system using a wavelet fuzzy neural network," *IEEE Trans. Fuzzy Systems*, vol. 22, no. 6, pp. 1598¡1611, 2014.

[28] V. I. Utkin and A. S. Poznyak, "Adaptive sliding mode control with application to super-twist algorithm: Equivalent control method," *Automatica*, vol. 49, no. 1, pp. 39¡47, 2013.

[29] Y. Wang, L. Gu, Y. Xu, and X. Cao, "Practical tracking control of robot manipulators with continuous fractional-order nonsingular terminal sliding mode," *IEEE Transactions on Industrial Electronics*, vol. 63, no. 10, pp. 6194¡6204, 2016.

[30] Z. Galias and X. Yu, "Dynamical behaviors of discretized second-order terminal sliding-mode control systems," *IEEE Transactions on Circuits and Systems II: Express Briefs*, vol. 59, no. 9, pp. 597¡601, 2012.

[31] M. J. Morshed and A. Fekih, "A fault-tolerant control paradigm for microgrid-connected wind energy systems," *IEEE Systems Journal*, vol.12, no. 1, pp. 360¡372, 2018.

[32] S. Nasiri and H. Seifi, "Robust probabilistic optimal voltage sag monitoring in presence of uncertainties," *ET Generation, Transmission & Distribution*, vol. 10, no. 16, pp. 4240¡4248, 2016.

[33] A. D. Hansen and G. Michalke, "Fault ride-through capability of DFIG wind turbines," *Renewable energy*, vol. 32, no. 9, pp. 1594¡1610, 2007.

[34] P.-H. Huang, M. S. El Moursi, and S. A. Hasen, "Novel fault ridethrough scheme and control strategy for doubly fed induction generatorbased wind turbine," *IEEE Transactions on Energy Conversion*, vol. 30, no. 2, pp. 635¡645, 2015.

[35] E. Bounadja, A. Djahbar, and Z. Boudjema, "Variable structure control of a doubly fed induction generator for wind energy conversion systems,"*Energy Procedia*, vol. 50, pp. 999¡1007, 2014.

[36] Z. Zhang, H. Zhang, Z. Wang, and Q. Shan, "Non-fragile exponential h-infinity control for a class of nonlinear networked control systems with short time-varying delay via output feedback controller," *IEEE transactions on cybernetics*, vol. 47, no. 8, pp. 2008¡2019, 2017.